

Atomas: Hierarchical Alignment on Molecule-Text for Unified Molecule Understanding and Generation

Yikun Zhang^{2†*}, Geyan Ye^{1††}, Chaohao Yuan³, Bo Han⁴, Long-Kai Huang¹,
Jianhua Yao¹, Wei Liu¹, Yu Rong^{1‡}

¹Tencent AI Lab

²Peking University

³Tsinghua University

⁴Hong Kong Baptist University

{yikun.zh,yu.rong}@hotmail.com, {blazerye,topliu}@tencent.com,
yuanch22@mails.tsinghua.edu.cn, bhanml@comp.hkbu.edu.hk,
{hlongkai,jianhua.yao}@gmail.com

Abstract

Molecule-and-text cross-modal representation learning has emerged as a promising direction for enhancing the quality of molecular representation, thereby improving performance in various scientific fields, including drug discovery and materials science. Existing studies adopt a global alignment approach to learn the knowledge from different modalities. These global alignment approaches fail to capture fine-grained information, such as molecular fragments and their corresponding textual description, which is crucial for downstream tasks. Furthermore, it is incapable to model such information using a similar global alignment strategy due to data scarcity of paired local part annotated data from existing datasets. In this paper, we propose Atomas, a multi-modal molecular representation learning framework to jointly learn representations from SMILES string and text. We design a Hierarchical Adaptive Alignment model to concurrently learn the fine-grained fragment correspondence between two modalities and align these representations of fragments in three levels. Additionally, Atomas’s end-to-end training framework incorporates the tasks of understanding and generating molecule, thereby supporting a wider range of downstream tasks. In the retrieval task, Atomas exhibits robust generalization ability and outperforms the baseline by 30.8% of recall@1 on average. In the generation task, Atomas achieves state-of-the-art results in both molecule captioning task and molecule generation task. Moreover, the visualization of the Hierarchical Adaptive Alignment model further confirms the chemical significance of our approach. Our codes can be found at <https://anonymous.4open.science/r/Atomas-03C3>.

1 Introduction

As a fundamental task, molecular representation learning holds significant importance across numerous biomedical fields, such as drug discovery [5, 20], virtual screening [33, 9], and molecular design [36, 32]. Recently, Molecule-and-Text cross-modal training models have made remarkable progress in the field of molecular representation learning [21, 25, 22]. These models improve the

*Work is done when Yikun Zhang worked as an intern in Tencent AI Lab.

†Equal contributions.

‡Yu Rong and Geyan Ye are the corresponding authors.

generalization ability of molecular representations by integrating information from various modalities, including textual description, SMILES string [21], structural data [22] and knowledge graph [25].

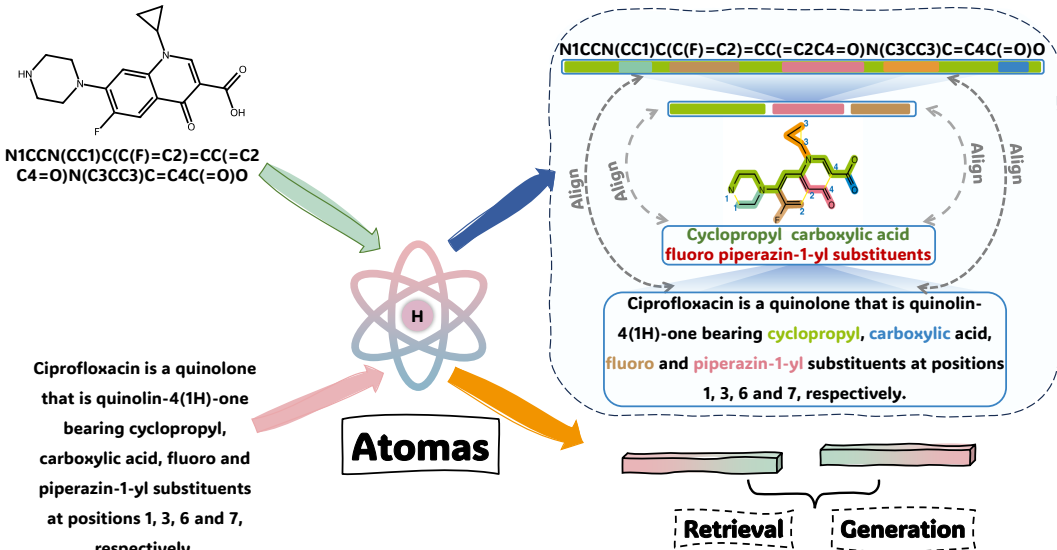


Figure 1: Atomas is a hierarchical, end-to-end cross-modal model for discovering and aligning local substructures of input modalities while performing conditional generation. The learned cross-modal representations can be adapted to both understanding tasks (retrieval tasks) and generation tasks.

The current cross-modal molecular representation learning approaches encounter three primary challenges. (1) Existing molecule-and-text alignment methods [4, 7, 21, 25, 22] struggle to effectively capture information of fine-grained correspondence related to local parts within different modalities, which is essential for downstream molecular tasks [35]. For instance, molecular fragments, which significantly influence molecular properties, are seldom described in molecular descriptions. Additionally, the lack of explicitly annotated paired local parts across molecule and text precludes the direct application of global alignment strategies to address fine-grained alignment challenges. (2) Current approaches [8, 37] primarily concentrate on developing alignment frameworks tailored for prediction tasks, overlooking the optimization of aligned representations for generative tasks. (3) The heterogeneity of different molecular modalities may result in overfitting during the alignment process due to the data scarcity within the molecular domain. For example, aligning text embeddings and structural embeddings is difficult, as they are generated by distinct types of encoders (transformers for texts and graph neural networks for structures) [11].

To address the aforementioned issues, we propose Atomas, a multi-modal molecular representation learning framework to jointly learn the representations from SMILES and text for molecule. Figure 1 given a conceptual illustration of Atomas. In Atomas, we exploit the unique characteristic of SMILES as a specialized form of text and employ a unified pre-trained encoder with the same architecture for both SMILES and text modalities as their base encoder. This unified encoder results in more isomorphic representations for both modalities, thereby facilitating subsequent alignment tasks. Meanwhile, to tackle the issue of local molecular alignment, we design a Hierarchical Adaptive Alignment (HAA) model which comprises two components: Adaptive Polymerization Module (APM) and Weighted Alignment Module (WAM). APM assigns the quantities of the low-level tokens into high-level tokens (fragments) for the single modality, while WAM leverages token representations from both SMILES and text modalities to automatically learn the matching of token and aligns the representation of two modalities in a set-wise manner. By iteratively invoking WAM and APM, we devised a three-level alignment scheme (atom level, fragment level, and molecule level). This hierarchical alignment structure enables improved learning of local alignment across different abstraction levels within the two modalities. Additionally, by incorporating a conditional decoder within the alignment process, Atomas can optimize the representation of molecule/text specifically for generation tasks. To validate the efficacy of Atomas, we conduct experiments on four typical retrieval and generation tasks spanning both SMILES and text modalities. In the molecule and text retrieval task, Atomas exhibits robust generalization ability and outperforms the baseline by 39.9% and 21.7% on recall@1, respectively. In the generation task, Atomas achieves state-of-the-art results in both

molecule captioning task and molecule generation task. Moreover, Atomas achieves consistently and significantly better performance than baseline methods under both the scaling of the training dataset and the scaling of the model size. These results confirm the superiority and robustness of Atomas compared to current existing approaches.

Our contributions are summarized as follows:

- To the best of our knowledge, Atomas is the pioneering multi-modal molecular representation learning framework that tackles the challenge of aligning local information across different modalities without the need for explicit labeling between text fragments and molecular substructures.
- In Atomas, we introduce the concept of Hierarchical Adaptive Alignment, enabling enhanced automatic learning of cross-modal local alignment information at different levels of abstractions.
- Atomas achieves state-of-the-art performance on a wide range of molecule-text tasks, including molecule and text retrieval, text-based de novo molecule generation, and molecule captioning.
- Atomas brings new insights into molecule conditional generation tasks: (1) Aligning before generation improves the performance of molecule conditional generation tasks. (2) Fine-grained alignment enhances the quality of controllable molecule generation. (3) Compared with two-stage training, the joint optimization training strategy is more beneficial to the molecular generation tasks.

2 Related Works

The primary challenge in multi-modal molecular representation learning is to effectively leverage information from various modalities to learn common representations shared between modalities, *i.e.*, aligning different modalities. Existing multi-modal molecule alignment approaches can be broadly categorized into two types: the internal modalities and the external modalities. The internal molecule structure representation includes 1D fingerprint and molecule string, specifically, SMILES (Simplified Molecular-Input Line-Entry System), 2D topological graph, and 3D conformational structure. The external functional description encompasses textual description and biological knowledge graph.

[7, 4, 23, 21, 25, 3] investigate the interaction between internal modalities and external modalities, *i.e.*, exchanging information between molecule structures and textual descriptions to complement the information between the two modalities and enhance the overall information content. All these methods only consider global representations of SMILES&text and overlook finer-grained modal interactions. Atomas first considers the hierarchical fine-grained alignment between SMILES and text, which is important in the molecular field for controlled molecule generation and molecular captioning, as it enables better performance. While [7, 4] treat conditional generation tasks akin to translation tasks without establishing alignment, Atomas highlights the efficacy of performing a preliminary alignment. In contrast to [23, 21, 25, 3]’s two-stage training strategies, Atomas presents a joint optimization approach, which is essential for the effective learning and generation of molecular representations.

[8, 37] focus on aligning intra-molecular modalities and tailoring for prediction tasks. Different from this alignment paradigms, Atomas addresses cross-modal learning between intra- and extra-molecular modalities. Challenges arise from the lack of expert fine-grained textual annotations for molecules and difficulty in constructing positive/negative pairs, as a text fragment may suit multiple molecule substructures. These challenges make Atomas’ achievements in this field particularly noteworthy.

3 Preliminaries

3.1 Molecule Representation

The structure of a molecule can be represented as a 1D molecular string. Specifically, SMILES is utilized to convert a chemical’s 3D structure into a string of symbols. For instance, the structure of a benzene ring can be represented as a SMILES string: C1=CC=C(C=C1). The 1D molecular string and the 2D graph are informationally equivalent, as SMILES can be losslessly converted

to a graph using chemical toolkits (e.g. RDKit). Furthermore, transformer-based encoder models exhibit less information loss compared to Graph Neural Networks (GNNs) [26], which suffer from over-smoothing problems, and GNNs cannot perform unified encoding with text modality, posing challenges for interaction between the two modalities. In this study, we choose the 1D SMILES string and textual description for molecule cross-modal representation learning.

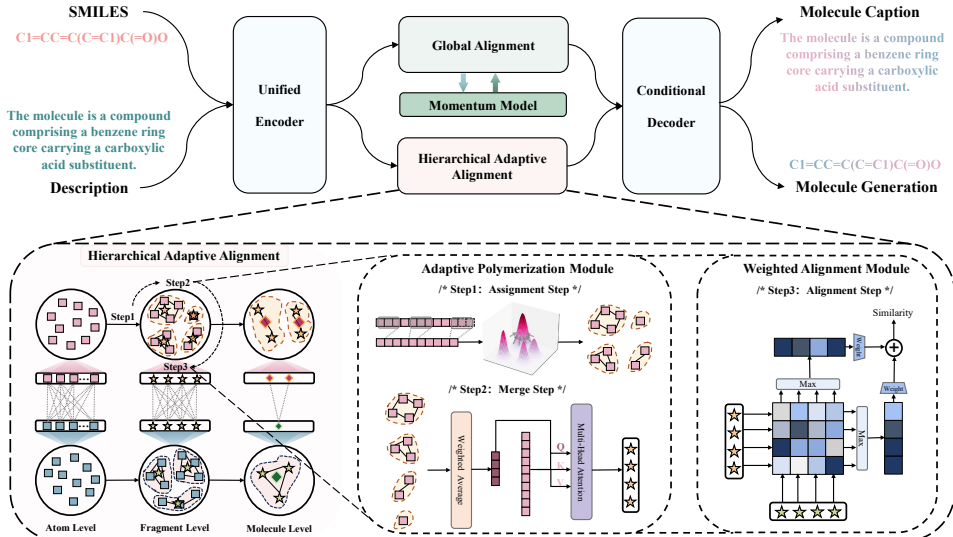


Figure 2: **Illustration of the proposed Atomas.** Atomas is composed of four components. (1) Unified Encoder encodes the input molecule and its corresponding textual description to the embeddings. (2) Global Alignment module projects the molecule and text to get the global features and align them in global-wise. To maintain alignment consistency, a momentum model is incorporated. (3) Hierarchical Adaptive Alignment aligns the molecule and text at three levels, including the Adaptive Polymerization module which clusters the original token features into a series of disentangled representation sets, and the Weighted Alignment module which aligns two modalities in a set-wise manner. (4) Conditional Decoder accepts the molecule and text embedding as input and generates the target modality.

3.2 Encoder-Decoder T5 Language Model

T5 [28] is an encoder-decoder transformer-based model. In the self-supervised pre-training stage, for the input sequence X , some words in the sequence are randomly chosen for corruption. Each consecutive span of corrupted tokens is masked by a sentinel token (e.g. $\langle x \rangle$, $\langle y \rangle$). Then the objective is to reconstruct the dropped-out spans:

$$\mathcal{L}_{mlm}(X; \theta) = \mathbb{E}_{x \sim X} \mathbb{E}_{\text{mask}} \sum_{i \in \text{mask}} \log p(x_i | x_{j \notin \text{mask}}; \theta).$$

We use a 12-layer T5 model as the backbone and initialized using MolT5 [7] weights, which have been pre-trained on both the textual modality C4 dataset [28] and the molecular modality ZINC dataset [30] in a self-supervised manner.

3.3 Density Peaks Clustering Algorithm

The Density Peaks Clustering Algorithm (DPC) [29] is a granular computing model that determines the number of clusters and their respective centers in a dataset by identifying density peaks. The algorithm is based on two assumptions. Assumption 1. The local density of cluster centers (density peaks) is greater than the local density of their surrounding neighbors. Assumption 2. The distance between different cluster centers is relatively large. Briefly, given a dataset $D = \{x_1, x_2, \dots, x_n\}$ with n samples, the local density of x_i is defined as $\rho_i = \sum_{j=1}^n \chi(d_{ij} - d_c)$, where χ is an indicator function: $\chi(x) = 1$ when $x < 0$, and $\chi(x) = 0$ otherwise, and d_c a cutoff distance. The relative

distance δ is defined as $\delta_i = \min_{j:\rho_j > \rho_i} (d_{ij})$. Based on ρ_i and δ , DPC algorithm constructs decision graphs to classify data points x_i as density peak points, normal points, or outliers.

4 The Atomas Method

4.1 Molecule-Text Unified Encoding

For a SMILES-text pair $M = (S, T)$, SMILES S and text description T are both fed into the unified encoder f_θ . We discuss the advantages of utilizing a unified encoder in Section 5.5. The input T with N_{ta} tokens is embedded into word sequence $\mathbf{T}_a = \{\mathbf{t}_a^i\}_{i=1}^{N_{ta}}$, where $\mathbf{t}_a^i \in \mathbb{R}^{D_t}$ denotes the feature vector of the i -th word. The input S with N_{sa} tokens is embedded into atom sequence $\mathbf{S}_a = \{\mathbf{s}_a^j\}_{j=1}^{N_{sa}}$, where $\mathbf{s}_a^j \in \mathbb{R}^{D_s}$. Since the T5 model does not have the [CLS] token, we first aggregate the \mathbf{T}_a and \mathbf{S}_a by a projection module $proj(\cdot)$ to obtain the global feature \mathbf{t}_g and \mathbf{s}_g :

$$\begin{aligned}\mathbf{t}_g &= proj(\mathbf{T}_a) = \mathbf{W}_t^\top \mathbf{T}_a + \mathbf{b}_t, \\ \mathbf{s}_g &= proj(\mathbf{S}_a) = \mathbf{W}_s^\top \mathbf{S}_a + \mathbf{b}_s,\end{aligned}\tag{1}$$

where $\mathbf{W}_t \in \mathbb{R}^{N_t \times 1}$ and $\mathbf{W}_s \in \mathbb{R}^{N_s \times 1}$ are the learned transformation matrix, \mathbf{b}_t and \mathbf{b}_s are the bias terms.

We then align the global representation pair $(\mathbf{t}_g, \mathbf{s}_g)$ by performing cross-modal contrastive learning. To ensure sufficient negative pairs and consistent feature representation from both modalities, we follow He et al. [10] to introduce a momentum unified encoder f_θ^m and two queues for text \mathbf{t} and SMILES \mathbf{s} denote as \mathbf{Q}_t and \mathbf{Q}_s , respectively. f_θ^m is updated by f_θ in the following way,

$$f_\theta^m \leftarrow \alpha f_\theta^m + (1 - \alpha) f_\theta,\tag{2}$$

where $\alpha \in [0, 1]$ is a momentum coefficient parameter and only the parameters f_θ are updated by back-propagation.

\mathbf{Q}_t and \mathbf{Q}_s store the global feature \mathbf{t}'_g and \mathbf{s}'_g generated by f_θ^m , thereby creating two large and consistent dictionaries that cover a rich set of negative samples. By doing this, we calculate the global similarity score of text-to-SMILES within the specified queue range instead of in a mini-batch:

$$S_g(\mathbf{t}, \mathbf{s}') = \frac{\exp(\text{sim}(\mathbf{t}_g, \mathbf{s}'_g)/\tau)}{\sum_{q=1}^Q \exp(\text{sim}(\mathbf{t}_g, \mathbf{Q}_s^q)/\tau)},\tag{3}$$

where τ is a learnable temperature parameter. and $\text{sim}(\cdot, \cdot)$ is the similarity metric, here we calculate it using the cosine similarity function. Similarly, we can obtain the global SMILES-to-text similarity score $S_g(\mathbf{s}, \mathbf{t}')$. Inspired by Li et al. [13, 14], soft labels are created from the momentum encoder f_θ^m as training targets to account for the potential positives in the negative pairs. Then the global alignment loss \mathcal{L}_{ga} can be formulated as:

$$\mathcal{L}_{ga} = -\frac{1}{2} \{ [(1 - \beta) \mathbf{y}^{t2s} + \beta S_g(\mathbf{t}', \mathbf{s}')] \log(S_g(\mathbf{t}, \mathbf{s}')) + [(1 - \beta) \mathbf{y}^{s2t} + \beta S_g(\mathbf{s}', \mathbf{t}')] \log(S_g(\mathbf{s}, \mathbf{t}')) \},\tag{4}$$

where β is a hyperparameter that controls the smoothness of the label. \mathbf{y}^{s2t} and \mathbf{y}^{t2s} denote the ground-truth one-hot similarity, denote the ground-truth one-hot similarity, where negative pairs have a probability of 0 and the positive pair has a probability of 1.

4.2 Hierarchical Adaptive Alignment

Given an encoded SMILES-text pair $M = (S, T)$, it is challenging to explicitly extract the corresponding fine-grained information (e.g., functional groups in SMILES and phrases in text) from \mathbf{S} and \mathbf{T} . To address this, we propose an **adaptive polymerization module** that clusters the original token-wise features into a series of disentangled representation sets. Subsequently, we introduce a **weighted alignment module** to estimate the correlation between the two modalities and identify potential active units in a set-wise manner.

Figure 2 illustrates the framework of hierarchical adaptive alignment. Adaptive polymerization module includes an assignment step and a merge step. Weighted alignment module performs the

alignment step. By stacking these two modules, we expand the fine-grained alignment between SMILES and text to the hierarchical interaction. We provide the experiment results of the effectiveness of hierarchical adaptive alignment in Table 4.

Specifically, we perform hierarchical adaptive alignment at three levels: **atom level**, where atom is aligned with word; **fragment level**, where functional group is aligned with phrase; and **molecule level**, where molecule is aligned with paragraph. Thus, the hierarchical adaptive alignment process alternates between three steps in a level-wise manner: assignment step, merge step, and alignment step.

Assignment Step We utilize a learnable token aggregation module to implement adaptive polymerization. The density peak-based clustering algorithm with k-nearest neighbors [6] (DPC-KNN) is utilized to assign tokens to clusters. Starting with the atom level, we firstly take atom (word) token features $S_a = \{s_a^j\}_{j=1}^{N_{sa}}$ into one-dimensional convolution to extract local features:

$$S_a = \text{LayerNorm}(\text{Conv}(S_a, \mathbf{W}, \mathbf{b}) + S_a). \quad (5)$$

Then we compute the local density ρ of each atom token feature s_a^j according to its k-nearest neighbors:

$$\rho_j = \exp \left(-\frac{1}{k} \sum_{s_a^i \in \text{KNN}(s_a^j)} \frac{\|s_a^i - s_a^j\|_2^2}{\sqrt{D_s}} \right) + \epsilon, \quad (6)$$

where s_a^i and s_a^j are their corresponding SMILES token features. D_s is the channel number of SMILES token features. $\text{KNN}(s_a^j)$ denotes the k-nearest neighbors of an atom token j . ϵ is a random noise that is randomly sampled from the uniform distribution within the interval $[0,1)$, ensuring that no tokens have the same density.

Then, we calculate the distance indicator δ for each token feature s_a^j by determining the minimum distance between it and any other token possessing a higher local density. As for the token with the highest local density, its indicator is determined as the maximum distance between it and any other tokens:

$$\delta_j = \begin{cases} \min_{i: \rho_i > \rho_j} \|s_a^i - s_a^j\|^2, & \text{if } \exists i \text{ s.t. } \rho_i > \rho_j \\ \max_i \|s_a^i - s_a^j\|^2, & \text{otherwise.} \end{cases} \quad (7)$$

Here, ρ serves as an indicator of the local density of tokens, which reflects the number of tokens located in the vicinity of s_a^j . δ represents the distance of a token from other high-density tokens, which measures how far it is from other tokens that are also located in highly dense regions. Together, ρ and δ provide valuable information about the distribution and proximity of $s_a^i \in S_a$.

We identify tokens with relatively high values of $\rho \times \delta$ as cluster centers and then assign all other tokens to their nearest cluster center based on the Euclidean distance d . This clustering approach enables us to decode the input tokens into coherent semantic units, providing a more structured and meaningful representation for both word sequence T_a and atom sequence S_a .

Merge Step Tokens with similar semantic meanings may not have equal importance, so in the merge step we first assign a weight to each token feature and calculate the weighted average token features of each cluster to represent the corresponding cluster:

$$S_m^j = \frac{\sum_{k=1}^{N_{sf}^j} w_k S_a^k}{\sum_{k=1}^{N_{sf}^j} w_k}, \quad (8)$$

where $w = \text{MLP}_\omega(S_a)$ is the weight of each token feature in S_a , N_{sf}^j means the set of the j -th SMILES cluster, S_a^k is the k -th token feature of S_a and w_k is the corresponding weight score. S_m^j is the j -th weighted average token feature.

Then we apply an attention mechanism on merged token features. S_m are used as queries Q and key K , value V corresponding to the original token features S_a . We take the resulting output of the attention module as a higher semantic level features, i.e., functional group sequence $S_f = \{s_f^j\}_{j=1}^{N_{sf}}$, where $s_f^j \in \mathbb{R}^{D_s}$. Perform the same operation of the above two steps on word tokens to get phrase

sequence $\mathbf{T}_f = \{\mathbf{t}_f^i\}_{i=1}^{N_{tf}}$, where $\mathbf{t}_f^i \in \mathbb{R}^{D_t}$, N_{tf} represents the number of clusters formed by word tokens. We repeat this process at the fragment level to obtain the molecule-level features.

Alignment Step After the assignment and merge steps, tokens are polymerized into semantic units. we perform the weighted alignment module Wang et al. [34] on each level in set-wise between the SMILES and text to get the weighted average maximum alignment score. Starting with the atom level, we can obtain the text-to-SMILES similarity score:

$$\mathbf{S}_{haa}^a(\mathbf{t}, \mathbf{s}) = \sum_{i=1}^{N_{ta}} \mathbf{w}_t^i(\mathbf{T}_a) \max_{j=1}^{N_{sa}} a_{ij}, \quad (9)$$

where $\mathbf{w}_t = \text{Softmax}(\text{MLP}_{\omega_t}(\mathbf{T}_a))$ represent the learnable weights for each textual token. The normalized alignment score $a_{ij} = \frac{(\mathbf{t}_a^i)^\top \mathbf{s}_a^j}{\|\mathbf{t}_a^i\|_2 \|\mathbf{s}_a^j\|_2}$ captures the similarity between the i -th description token feature and j -th SMILES token feature. Then the hierarchical adaptive alignment loss at the atom level can be calculated as:

$$\mathcal{L}_{haa}^a = -\frac{1}{2} \left[\frac{1}{B} \sum_k \log \frac{\exp(\mathbf{S}_{haa}^a(\mathbf{t}_k, \mathbf{s}_k)/\tau)}{\sum_l \exp(\mathbf{S}_{haa}^a(\mathbf{t}_k, \mathbf{s}_l)/\tau)} + \frac{1}{B} \sum_k \log \frac{\exp(\mathbf{S}_{haa}^a(\mathbf{s}_k, \mathbf{t}_k)/\tau)}{\sum_l \exp(\mathbf{S}_{haa}^a(\mathbf{s}_l, \mathbf{t}_k)/\tau)} \right], \quad (10)$$

where B is the batch size and τ is the temperature hyperparameter. The same alignment operation is performed on the fragment level and molecule level to get \mathcal{L}_{haa}^f and \mathcal{L}_{haa}^m .

4.3 Conditional Generation based on Aligned Representation

We employ a conditional generation approach to generate the target modality based on the aligned representations denoted as $\tilde{\mathbf{T}}_a = \{\tilde{\mathbf{t}}_a^i\}_{i=1}^{N_{ta}}$ and $\tilde{\mathbf{S}}_a = \{\tilde{\mathbf{s}}_a^j\}_{j=1}^{N_{sa}}$. In text-based molecule generation task, the decoder takes an aligned textual description $\tilde{\mathbf{T}}_a$ as input. The decoder then iteratively attends to previously generated tokens $\hat{\mathbf{s}}_a^{<j}$ via self-attention and input condition $\tilde{\mathbf{T}}_a$ via cross-attention. Using these attended representations, the decoder predicts the probability of future SMILES tokens $P(\hat{\mathbf{s}}_a^j | \hat{\mathbf{s}}_a^{<j}, \tilde{\mathbf{T}}_a)$. Then the decoder can be optimized by minimizing the negative log-likelihood of label SMILES \mathbf{s} tokens given textual description $\tilde{\mathbf{T}}_a$:

$$\mathcal{L}_{lm} = - \sum_{j=1}^{N_{sa}} \log P(\hat{\mathbf{s}}_a^j | \hat{\mathbf{s}}_a^{<j}, \tilde{\mathbf{T}}_a). \quad (11)$$

The same operation is applied to the molecule captioning task:

$$\mathcal{L}_{lm} = - \sum_{i=1}^{N_{ta}} \log P(\hat{\mathbf{t}}_a^i | \hat{\mathbf{t}}_a^{<i}, \tilde{\mathbf{S}}_a). \quad (12)$$

4.4 Training Objectives

During the training phase, we optimize three objective functions, consisting of the global alignment loss \mathcal{L}_{ga} , hierarchical adaptive alignment loss \mathcal{L}_{haa} , and language modeling loss \mathcal{L}_{lm} . Hierarchical adaptive alignment is performed at three semantic levels:

$$\mathcal{L}_{haa} = \mathcal{L}_{haa}^a + \mathcal{L}_{haa}^f + \mathcal{L}_{haa}^m, \quad (13)$$

where \mathcal{L}_{haa}^a , \mathcal{L}_{haa}^f , \mathcal{L}_{haa}^m operates at the atom level, fragment level, and molecule level, respectively.

The goal of Atomas is to align the molecule and text at different levels of granularity while conditionally reconstructing the molecule or text description. We jointly optimize these three objective functions in an end-to-end manner. The overall loss function of Atomas simultaneously:

$$\min_{\theta} \mathcal{L}_{ga} + \mathcal{L}_{haa} + \mathcal{L}_{lm}, \quad (14)$$

where θ denotes all learnable parameters of Atomas.

Table 1: **Performance comparison on molecule-text retrieval task.** **Bold** and underlined indicate the best and second-best results, respectively. R@1/5/10: Recall at 1/5/10; MRR: mean reversed rank. Details are provided in Appendix D.1.

Model	Text to Molecule				Molecule to Text			
	R@1	R@5	R@10	MRR	R@1	R@5	R@10	MRR
<i>1D SMILES + 2D Graph</i>								
MoMu	4.90	14.48	20.69	10.33	5.08	12.82	18.93	9.89
MolCA	35.09	<u>62.14</u>	<u>69.77</u>	47.33	<u>37.95</u>	66.81	74.48	<u>50.80</u>
<i>1D SMILES + 2D Graph + Knowledge Graph</i>								
MolFM	16.14	30.67	39.54	23.63	13.90	28.69	36.21	21.42
<i>1D SMILES</i>								
MoleculeSTM	35.80	-	-	-	39.50	-	-	-
Atomas-base (Ours)	<u>39.08</u>	59.72	66.56	<u>47.33</u>	37.88	59.22	65.56	47.81
Atomas-large (Ours)	49.08	68.32	73.16	57.79	46.22	<u>66.02</u>	<u>72.32</u>	55.52

Table 2: **Performance comparison on text-based de novo molecule generation.** **Bold** and underlined indicate the best and second-best results, respectively. “ \uparrow ” denotes that higher is better. “ \downarrow ” denotes that lower is better. Details are provided in Appendix D.1.

Model	BLEU \uparrow	Exact \uparrow	Levenshtein \downarrow	MACCS FTS \uparrow	RDKit FTS \uparrow	Morgan FTS \uparrow	Validity \uparrow
<i>1D SMILES + 2D Graph + 2D Image</i>							
GIT-Mol	0.756	0.051	26.32	0.738	0.582	0.519	0.928
<i>1D SMILES + 2D Graph + Knowledge Graph</i>							
MolFM-small	0.803	0.169	20.868	0.834	0.721	0.662	0.859
MolFM-base	0.822	0.210	19.45	0.854	0.758	0.758	0.892
<i>1D SMILES</i>							
MolT5-small	0.749	0.082	28.816	0.780	0.654	0.601	0.725
MolT5-base	0.779	0.082	25.19	0.788	0.662	0.602	0.787
MolT5-large	0.854	0.318	16.32	0.889	0.813	0.750	0.958
Text+Chem T5-augm	0.853	0.322	16.87	0.901	0.816	0.757	0.943
MolXPT	-	0.215	-	0.859	0.757	0.667	0.983
MolReGPT (GPT-3.5-turbo)	0.790	0.139	24.91	0.847	0.708	0.624	0.887
MolReGPT (GPT-4-0413)	0.857	0.280	17.14	0.903	0.805	0.739	0.899
Atomas-base (Ours)	<u>0.868</u>	<u>0.343</u>	<u>13.76</u>	<u>0.908</u>	<u>0.827</u>	<u>0.773</u>	<u>0.971</u>
Atomas-large (Ours)	0.870	0.376	13.35	0.911	0.835	0.782	0.965

5 EXPERIMENTS

In this section, we present the quantitative and qualitative results of Atomas. The experiment is set to evaluate the effectiveness of Atomas in three aspects: (1) improving the alignment efficiency of **retrieval tasks**, (2) enhancing the generation capability of **generation tasks**, and (3) evaluating the **effectiveness of each module in Atomas**.

5.1 Initial Training

Training Dataset We collect 280K molecular SMILES-text pairs from PubChem website and follow the MoleculeSTM’s [21] pipeline to construct the dataset. Subsequently, we combine pairs with the same PubChem ID, resulting in 243K unique pairs. Textual descriptions with fewer than 18 characters are filtered out, and to prevent data leakage, we remove duplicates from the datasets used in downstream tasks. This process result in a high-quality, leak-free dataset of 51,340 pairs. We then train the Atomas on this refined dataset and evaluate its performance in the zero-shot setting and fine-tune it for various downstream tasks. The details of dataset construction and statistics are provided in Appendix B.1.

Training Details We train the model on 8 NVIDIA Tesla A100-SXM4-40GB GPUs using a batch size of 16 SMILES-text pairs, no weight decay, and the learning rate is set to $1e-4$. The momentum parameter α for updating the momentum model is set to 0.995, and the size of the queue Q used for global SMILES-text pair contrastive learning is set to 13200. The label smooth weight β is set to 0.4. More implementation details are provided in Appendix C.

Table 3: **Performance comparison on molecule captioning task.** **Bold** and underlined indicate the best and second-best results, respectively. Our Atomas achieves superior performance within the methods utilizing 1D SMILES, surpassing even those employing two or more modalities. Details are provided in Appendix D.1.

Model	#Params	BLEU-2	BLEU-4	ROUGE-1	ROUGE-2	ROUGE-L
<i>1D SMILES + 2D Graph</i>						
MoMu-small	82M	0.532	0.445	-	-	0.564
MoMu-base	252M	0.549	0.462	-	-	0.575
MoMu-large	782M	0.599	0.515	-	-	0.593
InstructMol-GS	6.9B	0.475	0.371	0.566	0.394	0.502
MolCA, Galac1.3B	1.3B	0.620	0.531	0.681	0.537	0.618
<i>1D SMILES + 2D Graph + Image</i>						
GIT-Mol-GS	700M	0.352	0.263	0.575	0.485	0.560
<i>1D SMILES + 2D Graph + Knowledge Graph</i>						
MolFM-small	136.2M	0.542	0.452	0.623	0.469	0.562
MolFM-base	296.2M	0.585	0.498	0.653	0.508	0.594
<i>1D SMILES</i>						
MolT5-small	77M	0.519	0.436	0.620	0.469	0.563
MolT5-base	248M	0.540	0.457	0.634	0.485	0.578
MolT5-large	783M	0.594	0.508	0.654	0.510	0.594
Text+Chem T5-augm	220M	<u>0.625</u>	<u>0.542</u>	<u>0.682</u>	<u>0.543</u>	<u>0.622</u>
MolXPT	350M	0.594	0.505	0.660	0.511	0.597
MolReGPT (GPT-3.5-turbo)	>175B	0.565	0.482	0.450	0.543	0.585
MolReGPT (GPT-4-0314)	-	0.607	0.525	0.634	0.476	0.562
Atomas-base w/o initial training (Ours)	271M	0.604	0.518	0.674	0.531	0.615
Atomas-base (Ours)	271M	0.632	0.548	0.684	0.546	0.625

5.2 Molecule-Text Retrieval

Dataset and Metric To evaluate the performance of our retrieval experiment, we utilize the PCdes [38] dataset, which comprises 15,000 molecule pairs collected from PubChem. Following the previous work by MolFM [25], we exclude eight molecules whose SMILES strings could not be converted into 2D graphs using RDKit, leaving us with 14,992 instances. We employ scaffold splitting to partition the dataset into training, validation, and test sets at a ratio of 7:1:2. We use MRR (Mean Reciprocal Rank) and Recall at 1/5/10 as metrics for this task. For inference, we perform retrieval directly across the entire test dataset, without the preliminary selection of a top-k candidate set.

Results Table 1 shows that our Atomas exhibits superior performance in both text-to-molecule retrieval and molecule-to-text retrieval tasks, compared to other recently proposed state-of-the-art methods. Atomas outperforms the global alignment-based baseline by 39.9% and 21.7% on recall@1 scores in the two retrieval tasks. This result suggests that performing multi-level fine-grained interaction and alignment could lead to much better results than methods that rely solely on coarse-grained representations. Detailed introduction to the baselines can be found in Appendix D.2.

5.3 Text-based de Novo Molecule Generation

Dataset and Metric ChEBI-20 [7] is a widely recognized gold standard dataset that has been extensively used for molecular generation tasks in the field of deep learning and molecular biology. The dataset comprises 33,010 molecule-description pairs and is separated into 80/10/10% train/validation/test splits. To assess our model’s performance, we adopt standard metrics commonly used in generation task, including BLEU, exact ratio, valid ratio, Levenshtein distance, and fingerprint tanimoto similarity (MACCS fingerprint, Morgan fingerprint, RDKit fingerprint). We present more details in Appendices B and D.1.

Quantitative Results Table 2 summarizes the overall text-based de novo molecule generation performance. Atomas outperforms all baseline models in six out of seven metrics, except for the validity metric. In contrast to our work, these methods [17, 25] utilize independent unimodal pre-trained models to encode different modalities and learn a joint embedding space. However, these methods fail to consider that employing separate encoders complicates the exchange of information between modalities. They do not facilitate fine-grained interactions between different modalities, and the two-stage training process constrains their generative capabilities. Additionally, GPT-like and encoder-decoder-based methods [7, 4, 24, 16] neglect the benefits that can be derived from properly aligned multimodal representation.

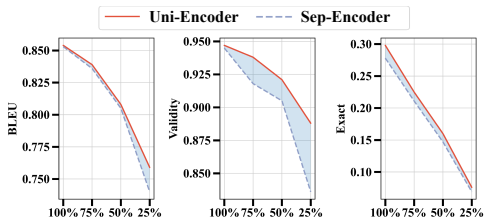


Figure 3: **Unified encoder vs separate encoder.** We perform weighted sampling of 75%, 50%, and 25% of the training set (100%) as training subsets and evaluate the performance of molecule generation task on the original validation and test sets.

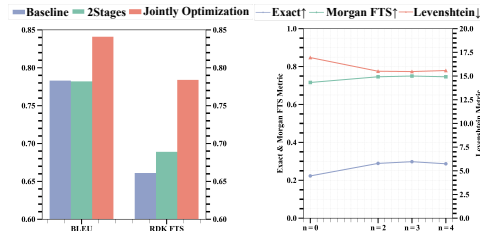


Figure 4: **Ablation study for the effectiveness of joint optimization** on molecule generation task using ChEBI-20 dataset (left) and **the effect of different number of hierarchical alignment levels** (right).

Table 4: **Ablation study for the effectiveness of components on molecule generation task.** The first row is the baseline without alignment to generate SMILES based on text. The second row is the baseline without using the hierarchical alignment. Complete indicators are in the Appendix E.2

\mathcal{L}_{ga}	\mathcal{L}_{haa}	\mathcal{L}_{lm}	Exact \uparrow	Levenshtein \downarrow	Morgan FTS \uparrow
		✓	0.082	24.846	0.602
✓		✓	0.223	16.946	0.716
	✓	✓	0.266	16.675	0.736
✓	✓	✓	0.298	15.472	0.750

Table 5: **Ablation study for the effectiveness of joint optimization on molecule retrieval task.**

Training Strategy	Text to Molecule			
	R@1	R@5	R@10	MRR
2Stages	37.74	58.01	65.02	47.20
Joint optimization	39.08	59.72	66.56	48.47

Training Strategy	Molecule to Text			
	R@1	R@5	R@10	MRR
2Stages	36.54	57.31	63.58	46.10
Joint optimization	37.88	59.22	65.56	47.81

5.4 Molecule Captioning

Dataset and Metric We evaluate Atomas for molecule generation using the ChEBI-20 dataset. Evaluation metrics include BLEU-2, BLEU-4, ROUGE-1, ROUGE-2, and ROUGE-L. We present more details in Appendices B and D.1.

Quantitative Results Table 3 shows the overall molecule captioning performance. It shows that Atomas outperforms all baseline methods across all evaluation metrics. Our Atomas-base model performs much better than the MolT5-large model, using only 35.0% of its parameters and no initial training, demonstrating the superiority of our proposed framework. Furthermore, despite utilizing 1D SMILES, Atomas still achieves the best performance in the caption generation task. The results demonstrate the effectiveness of Atomas in modeling the interaction between SMILES and text.

5.5 Ablation Study

Unified encoder better than separate encoders: To investigate the impact of using a unified encoder versus two separate encoders for text and SMILES, we conduct experiments on the molecule generation task. Specifically, we perform weighted sampling of 75%, 50%, and 25% of the training set as training subsets based on the distribution of text lengths, and evaluate the performance on the original validation and test sets. As shown in Figure 3, as the size of the training sets decreases, the performance of the separate encoders (Sep-Encoder) significantly declines compared to the unified encoder (Uni-Encoder). These findings have important implications for the field of molecular design, where data scarcity is a common challenge. The complete performance details can be found in Appendix E.1.

The effectiveness of components: Table 4 shows the ablation study for the architecture design on the molecule generation task. The first row is the baseline without alignment to generate SMILES based on text. The second row is the baseline without using the hierarchical alignment. The results show that the full model achieves the best performance and outperforms the baseline by 21.6% at Exact, 9.47% at Levenshtein and 14.8% at Morgan FTS. This demonstrates that performing hierarchical cross-modal interaction and alignment could lead to much better results.

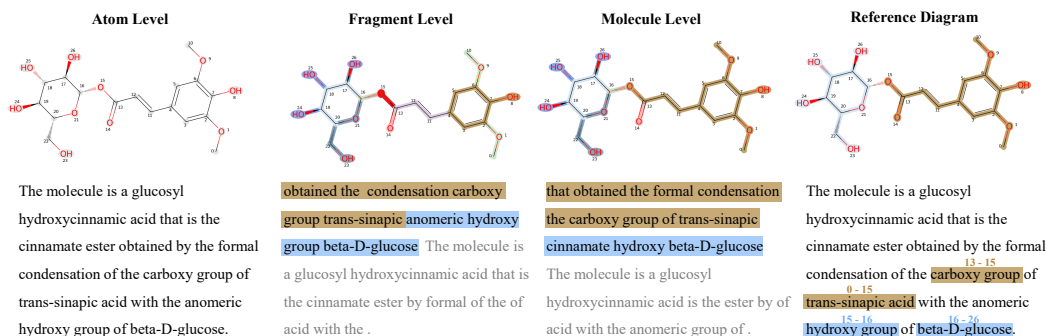


Figure 5: **The visualization of adaptive polymerization module.** The process of atom (word) polymerization to form individual sets is illustrated at three levels, including the reference diagram, from left to right. Atoms (words) belonging to the same set are highlighted using the same color.

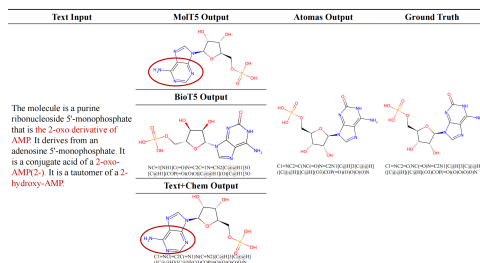


Figure 6: **A sample of molecule generation.**

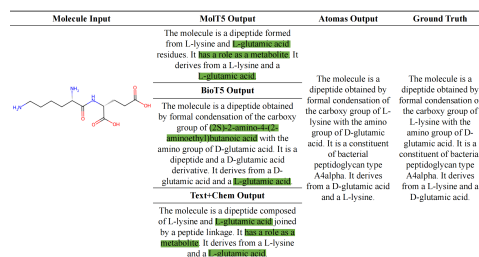


Figure 7: **A sample of molecule captioning.**

Joint optimization benefits both learned representation quality and generation task performance: Table 5 and Figure 4 (left) show the ablation study on molecule retrieval and generation task for the different training strategies. The “Baseline” refers to the MolT5-base model. From these results, we can conclude that the essence of joint optimization is the mutual facilitation between the caption/generation task and molecular representation learning (retrieval tasks). From model perspective: As suggested by the existing study [1], attention-based generation tasks essentially perform a form of soft alignment. During the generation process, the attention mechanism facilitates a mutual translation between text and SMILES, reinforcing the semantic consistency between the textual description and the molecular structure it represents. Concurrently, representation learning bridges the domain gap between text and SMILES, enhancing the caption/generation task. From data perspective: The captioning and generation tasks may provide complementary information for learning molecular representations. These tasks necessitate the model to learn the mapping between text and molecular domains, which allows the model to grasp the intricate relationship between textual descriptions and molecular structures, thereby enriching the quality of the learned molecular representations. Hierarchical alignment further aids in capturing local data pair relationships, benefiting the generation process.

The effect of hierarchical alignment level numbers We further analyze the effect of adaptive alignment level numbers. The results are shown in Figure 4 (right). We find that the model achieves the best performance at 3-level numbers.

5.6 Visualization and Qualitative Analysis

Visualization To better understand the proposed method, we present the visualization of the adaptive polymerization module in Figure 5. The molecule in the figure is formed by combining atoms at positions 0-15 and at sites 16-26 through dehydration condensation. At the atom level, individual atoms are aligned with words. At the fragment level, Atomas clusters atoms (words) with similar semantics into functional groups (phrases) using an adaptive polymerization module. At the molecule level, Atomas further clusters functional groups into monomers, emphasizing information at the molecular level. As shown in Figure 5, from fragment level to molecule level, Atomas clusters atoms

Table 6: **The scaling of the initial training dataset on molecule generation task** Here we choose 15k training data to be consistent with MolFM which is one of the baselines in the paper.

Model	Data sizes	BLEU \uparrow	Exact \uparrow	Levenshtein \downarrow	MACCS FTS \uparrow	RDKit FTS \uparrow	Morgan FTS \uparrow	Validity \uparrow
Atomas-base	0	0.854	0.298	15.47	0.898	0.809	0.750	0.947
Atomas-base	15k	0.861	0.318	14.68	0.902	0.817	0.757	0.965
Atomas-base	51k	0.868	0.343	13.76	0.908	0.827	0.773	0.971

Table 7: **The scaling of the model size on molecule generation task** The results presented below demonstrate that increasing the parameters of Atomas can lead to further improvements generation performance.

Model	Model sizes	BLEU \uparrow	Exact \uparrow	Levenshtein \downarrow	MACCS FTS \uparrow	RDKit FTS \uparrow	Morgan FTS \uparrow	Validity \uparrow
MolReGPT (GPT-3.5-turbo)	>175B	0.790	0.139	24.91	0.847	0.708	0.624	0.887
MolReGPT (GPT-4-0413)	>175B	0.857	0.280	17.14	0.903	0.805	0.739	0.899
MolT5-base	248M	0.779	0.082	25.19	0.788	0.662	0.602	0.787
MolT5-large	783M	0.854	0.318	16.32	0.889	0.813	0.750	0.958
Atomas-base	271M	0.868	0.343	13.76	0.908	0.827	0.773	0.971
Atomas-large	825M	0.870	0.376	13.35	0.911	0.835	0.782	<u>0.965</u>

at sites 0-13 and 15 together to form a monomer-like structure. This indicates that Atomas is more inclined towards focusing on macro-level information as it ascends the hierarchy.

Qualitative Analysis In Figure 6, we can see that [4, 7] generate the ‘AMP’ structure, but neglect the fine-grained information ‘2-hydroxy’. Conversely, Atomas can successfully generate the ‘2-hydroxy-AMP’ structure, which highlights the significance of hierarchical alignment in capturing the relationship between molecular substructures and textual fragments. As shown in Figure 7, [4, 7, 27] are all insufficient in distinguishing between the ‘D-glutamate’ and ‘L-glutamate’ enantiomers, indicating they failed to accurately capture their stereochemical differences. This oversight can lead to significant inaccuracies in chemical analysis and interpretation. In contrast, Atomas successfully generates a more comprehensive and accurate description of molecules. This highlights the usefulness of hierarchical alignment models in improving molecule captioning task.

5.7 The Scalability and Robustness of Atomas.

We conducted two scaling experiments to show Atomas’s scalability and robustness. As can be seen from the Table 6 and Table 7, Atomas achieves consistently and significantly better performance than baseline methods under both the scaling of the training dataset and the scaling of the model size.

6 Conclusion

In this paper, we proposed an innovative hierarchical alignment framework Atomas that addresses the limitations of existing methods by incorporating an adaptive polymerization module and a weighted alignment module to learn fine-grained information between molecules and texts. This approach not only captures information at multiple levels of detail but also simplifies the application of cross-modal representation in downstream tasks by integrating the tasks of understanding and generating molecules. The robustness and effectiveness of the framework are demonstrated through its successful application in molecule retrieval, molecule captioning, and molecule generation. Future research could further explore and enhance this innovative approach to cross-modal representation learning.

References

- [1] D. Bahdanau, K. H. Cho, and Y. Bengio. Neural machine translation by jointly learning to align and translate. In *3rd International Conference on Learning Representations, ICLR 2015*, 2015.
- [2] H. Cao, Z. Liu, X. Lu, Y. Yao, and Y. Li. Instructmol: Multi-modal integration for building a versatile and reliable molecular assistant in drug discovery. *arXiv preprint arXiv:2311.16208*, 2023.
- [3] Z. Chen, Y. Zhang, Y. Fang, Y. Geng, L. Guo, X. Chen, Q. Li, W. Zhang, J. Chen, Y. Zhu, et al. Knowledge graphs meet multi-modal learning: A comprehensive survey. *arXiv preprint arXiv:2402.05391*, 2024.
- [4] D. Christofidellis, G. Giannone, J. Born, O. Winther, T. Laino, and M. Manica. Unifying molecular and textual representations via multi-task language modelling. In *International Conference on Machine Learning*, pages 6140–6157. PMLR, 2023.
- [5] J. Drews. Drug discovery: a historical perspective. *science*, 287(5460):1960–1964, 2000.
- [6] M. Du, S. Ding, and H. Jia. Study on density peaks clustering based on k-nearest neighbors and principal component analysis. *Knowledge-Based Systems*, 99:135–145, 2016. ISSN 0950-7051. doi: <https://doi.org/10.1016/j.knosys.2016.02.001>. URL <https://www.sciencedirect.com/science/article/pii/S0950705116000794>.
- [7] C. Edwards, T. Lai, K. Ros, G. Honke, K. Cho, and H. Ji. Translation between molecules and natural language. In Y. Goldberg, Z. Kozareva, and Y. Zhang, editors, *Proceedings of the 2022 Conference on Empirical Methods in Natural Language Processing*, pages 375–413, Abu Dhabi, United Arab Emirates, Dec. 2022. Association for Computational Linguistics. doi: 10.18653/v1/2022.emnlp-main.26. URL <https://aclanthology.org/2022.emnlp-main.26>.
- [8] S. Feng, L. Yang, W. Ma, and Y. Lan. Unimap: Universal smiles-graph representation learning. *arXiv preprint arXiv:2310.14216*, 2023.
- [9] M. Goel, R. Aggarwal, B. Sridharan, P. K. Pal, and U. D. Priyakumar. Efficient and enhanced sampling of drug-like chemical space for virtual screening and molecular design using modern machine learning methods. *Wiley Interdisciplinary Reviews: Computational Molecular Science*, 13(2):e1637, 2023.
- [10] K. He, H. Fan, Y. Wu, S. Xie, and R. Girshick. Momentum contrast for unsupervised visual representation learning. In *Proceedings of the IEEE/CVF conference on computer vision and pattern recognition*, pages 9729–9738, 2020.
- [11] A. Kalinowski and Y. An. A survey of embedding space alignment methods for language and knowledge graphs. *arXiv preprint arXiv:2010.13688*, 2020.
- [12] J. D. M.-W. C. Kenton and L. K. Toutanova. Bert: Pre-training of deep bidirectional transformers for language understanding. In *Proceedings of NAACL-HLT*, pages 4171–4186, 2019.
- [13] J. Li, R. Selvaraju, A. Gotmare, S. Joty, C. Xiong, and S. C. H. Hoi. Align before fuse: Vision and language representation learning with momentum distillation. *Advances in neural information processing systems*, 34:9694–9705, 2021.
- [14] J. Li, D. Li, C. Xiong, and S. Hoi. Blip: Bootstrapping language-image pre-training for unified vision-language understanding and generation. In *International Conference on Machine Learning*, pages 12888–12900. PMLR, 2022.
- [15] J. Li, D. Li, S. Savarese, and S. Hoi. Blip-2: Bootstrapping language-image pre-training with frozen image encoders and large language models. In *International conference on machine learning*, pages 19730–19742. PMLR, 2023.
- [16] J. Li, Y. Liu, W. Fan, X.-Y. Wei, H. Liu, J. Tang, and Q. Li. Empowering molecule discovery for molecule-caption translation with large language models: A chatgpt perspective. *arXiv preprint arXiv:2306.06615*, 2023.

- [17] P. Liu, Y. Ren, and Z. Ren. Git-mol: A multi-modal large language model for molecular science with graph, image, and text. *arXiv preprint arXiv:2308.06911*, 2023.
- [18] P. Liu, Y. Ren, J. Tao, and Z. Ren. Git-mol: A multi-modal large language model for molecular science with graph, image, and text. *Computers in Biology and Medicine*, 171:108073, 2024. ISSN 0010-4825. doi: <https://doi.org/10.1016/j.compbiomed.2024.108073>. URL <https://www.sciencedirect.com/science/article/pii/S0010482524001574>.
- [19] S. Liu, H. Wang, W. Liu, J. Lasenby, H. Guo, and J. Tang. Pre-training molecular graph representation with 3d geometry. In *International Conference on Learning Representations*, 2022. URL <https://openreview.net/forum?id=xQe1pOKPam>.
- [20] S. Liu, H. Guo, and J. Tang. Molecular geometry pretraining with SE(3)-invariant denoising distance matching. In *The Eleventh International Conference on Learning Representations*, 2023. URL <https://openreview.net/forum?id=CjTHVo1dvR>.
- [21] S. Liu, W. Nie, C. Wang, J. Lu, Z. Qiao, L. Liu, J. Tang, C. Xiao, and A. Anandkumar. Multi-modal molecule structure-text model for text-based retrieval and editing. *Nature Machine Intelligence*, 5(12):1447–1457, 2023.
- [22] Z. Liu, S. Li, Y. Luo, H. Fei, Y. Cao, K. Kawaguchi, X. Wang, and T.-S. Chua. MolCA: Molecular graph-language modeling with cross-modal projector and uni-modal adapter. In H. Bouamor, J. Pino, and K. Bali, editors, *Proceedings of the 2023 Conference on Empirical Methods in Natural Language Processing*, pages 15623–15638, Singapore, Dec. 2023. Association for Computational Linguistics. doi: 10.18653/v1/2023.emnlp-main.966. URL <https://aclanthology.org/2023.emnlp-main.966>.
- [23] Z. Liu, S. Li, Y. Luo, H. Fei, Y. Cao, K. Kawaguchi, X. Wang, and T.-S. Chua. Molca: Molecular graph-language modeling with cross-modal projector and uni-modal adapter. *arXiv preprint arXiv:2310.12798*, 2023.
- [24] Z. Liu, W. Zhang, Y. Xia, L. Wu, S. Xie, T. Qin, M. Zhang, and T.-Y. Liu. MolXPT: Wrapping molecules with text for generative pre-training. In A. Rogers, J. Boyd-Graber, and N. Okazaki, editors, *Proceedings of the 61st Annual Meeting of the Association for Computational Linguistics (Volume 2: Short Papers)*, pages 1606–1616, Toronto, Canada, July 2023. Association for Computational Linguistics. doi: 10.18653/v1/2023.acl-short.138. URL <https://aclanthology.org/2023.acl-short.138>.
- [25] Y. Luo, K. Yang, M. Hong, X. Liu, and Z. Nie. Molfm: A multimodal molecular foundation model. *arXiv preprint arXiv:2307.09484*, 2023.
- [26] H. Ma, Y. Bian, Y. Rong, W. Huang, T. Xu, W. Xie, G. Ye, and J. Huang. Cross-dependent graph neural networks for molecular property prediction. *Bioinformatics*, 38(7):2003–2009, 2022.
- [27] Q. Pei, W. Zhang, J. Zhu, K. Wu, K. Gao, L. Wu, Y. Xia, and R. Yan. BioT5: Enriching cross-modal integration in biology with chemical knowledge and natural language associations. In H. Bouamor, J. Pino, and K. Bali, editors, *Proceedings of the 2023 Conference on Empirical Methods in Natural Language Processing*, pages 1102–1123, Singapore, Dec. 2023. Association for Computational Linguistics. doi: 10.18653/v1/2023.emnlp-main.70. URL <https://aclanthology.org/2023.emnlp-main.70>.
- [28] C. Raffel, N. Shazeer, A. Roberts, K. Lee, S. Narang, M. Matena, Y. Zhou, W. Li, and P. J. Liu. Exploring the limits of transfer learning with a unified text-to-text transformer. *Journal of machine learning research*, 21(140):1–67, 2020.
- [29] A. Rodriguez and A. Laio. Clustering by fast search and find of density peaks. *science*, 344(6191):1492–1496, 2014.
- [30] T. Sterling and J. J. Irwin. Zinc 15–ligand discovery for everyone. *Journal of chemical information and modeling*, 55(11):2324–2337, 2015.

- [31] B. Su, D. Du, Z. Yang, Y. Zhou, J. Li, A. Rao, H. Sun, Z. Lu, and J.-R. Wen. A molecular multimodal foundation model associating molecule graphs with natural language. *arXiv preprint arXiv:2209.05481*, 2022.
- [32] M. Thomas, A. Bender, and C. de Graaf. Integrating structure-based approaches in generative molecular design. *Current Opinion in Structural Biology*, 79:102559, 2023.
- [33] W. P. Walters, M. T. Stahl, and M. A. Murcko. Virtual screening—aan overview. *Drug discovery today*, 3(4):160–178, 1998.
- [34] Q. Wang, Y. Zhang, Y. Zheng, P. Pan, and X.-S. Hua. Disentangled representation learning for text-video retrieval. *arXiv preprint arXiv:2203.07111*, 2022.
- [35] J. Xia, L. Zhang, X. Zhu, Y. Liu, Z. Gao, B. Hu, C. Tan, J. Zheng, S. Li, and S. Z. Li. Understanding the limitations of deep models for molecular property prediction: Insights and solutions. In *Thirty-seventh Conference on Neural Information Processing Systems*, 2023. URL <https://openreview.net/forum?id=NLFqlDeuzt>.
- [36] G. Ye, X. Cai, H. Lai, X. Wang, J. Huang, L. Wang, W. Liu, and X. Zeng. Drugassist: A large language model for molecule optimization. *arXiv preprint arXiv:2401.10334*, 2023.
- [37] Q. Yu, Y. Zhang, Y. Ni, S. Feng, Y. Lan, H. Zhou, and J. Liu. Multimodal molecular pretraining via modality blending. In *The Twelfth International Conference on Learning Representations*, 2024. URL <https://openreview.net/forum?id=oM7Jbxdk6Z>.
- [38] Z. Zeng, Y. Yao, Z. Liu, and M. Sun. A deep-learning system bridging molecule structure and biomedical text with comprehension comparable to human professionals. *Nature communications*, 13(1):862, 2022.

A Comparison to Related Works

A.1 Text guided conditional Molecule Generation

Text-based molecule generation models can be primarily categorized into two types. One type uses a decoder-only transformer architecture, such as MolXPT [24]. This is a GPT-like model that utilizes the GPT-2_{medium} configuration, which has been pre-trained on SMILES sequences encapsulated by text. The second type employs an encoder-decoder transformer architecture. This type translates between text and molecule strings, and it can adapt to the text-conditional de novo generation. Models like MolT5 and Text+Chem T5 [4] work by jointly encoding the molecule string and natural language. They then use the input description to generate a molecule string.

In Table 8, we provide a comprehensive overview of existing works on molecule-text alignment methods. We have identified two key distinctions from existing methods: (i) Current contrastive learning-based alignment methods primarily align global features, neglecting finer-grained modal interactions. Fine-grained alignment is important in tasks such as controlled molecule generation and molecular captioning, as it enables greater precision and accuracy. (ii) Existing end-to-end training methods use conditional generation to create molecules, without aligning the molecule modality and text modality. However, our experimental results demonstrate that performing alignment before conditional generation can significantly improve generation performance.

Table 8: Comparison between Atomas and existing multimodal molecule alignment methods.

Model	Alignment				Task			Training Strage	
	Text	Molecule			Molecule Retrieval	Molecule Generation	Molecule Caption	Multi-Stage	End-to-End
		1D	2D	3D					
MoMu [31]	✓	✓	✓	-	✓	✓	✓	✓	-
KV-PLM [38]	✓	✓	-	-	✓	-	-	✓	-
GraphMVP [19]	-	✓	✓	✓	✓	-	-	-	✓
InstructMol [2]	✓	✓	✓	-	-	-	✓	✓	-
MolCA [22]	✓	✓	✓	-	✓	-	✓	✓	-
GIT-Mol [18]	✓	✓	✓	-	✓	✓	-	✓	-
MolFM [25]	✓	✓	✓	-	✓	✓	✓	✓	-
MolT5 [7]	✓	✓	-	-	-	✓	✓	-	✓
Text+Chem T5 [4]	✓	✓	-	-	-	✓	✓	-	✓
MolXPT [24]	✓	✓	-	-	-	✓	✓	✓	-
MolReGPT [16]	✓	✓	-	-	-	✓	✓	-	-
MoleculeSTM [21]	✓	✓	✓	-	✓	-	-	✓	-
Atomas (Ours)	✓	✓	-	-	✓	✓	✓	-	✓

B Data Details

B.1 Initial Training Dataset Construction

We obtain a dataset of 280K molecule-text pairs from PubChem database and follow the MolecularSTM to preprocess the textual descriptions, named PubchemSTM-raw. Molecule names are replaced by “This molecule is ...” or “These molecules are” to prevent the model from identifying molecules by name alone. To create unique SMILES-text pairs, molecules with the same CID (Chemical Identifier) are combined, resulting in 243K pairs. Text descriptions with less than 18 characters are filtered out, resulting in a set of 64,285 samples. In order to avoid data leakage, we removed duplicates from the ChEBI-20 and PCdes datasets used in downstream tasks. Specifically, we first convert the smiles string into a canonical SMILES string using the RDKit toolkit, and then de-duplicate the initial training dataset with the same SMILES string as the ChEBI-20 dataset and PCdes datasets, respectively. This resulted in a high-quality and leak-free dataset of 51,340 pairs, named PubchemSTM-distll. It should be noted that PubchemSTM-distll is used exclusively for initial training and does not divide the training, testing, and validation sets.

B.2 Dataset Statistic

Table 9 presents the dataset statistics. We observe that PubchemSTM-raw includes many uninformative texts; for example, some descriptions include just one word, such as “4,4’-Methylenebis”. and one molecule corresponds to multiple descriptions. So, we first create unique SMILES-text pairs by grouping pairs by CID, and then filter out the texts with a length of less than 18 characters.

Table 9: Statistics of the datasets.

Dataset	Molecule-Text Pair	Train	Valid	Test	Min Word	Avg Word	Median Word
PubchemSTM-raw	280011	-	-	-	1	18.37	13
PubchemSTM-distll	51340	51340	0	0	18	44.64	30
ChEBI-20	33008	26407	3301	3300	18	43.49	40
PCdes	14995	10495	1500	3000	17	61.2	50

B.3 Dataset Examples

Figure 8 shows some examples of our dataset. To make it easier to understand, we use the RDKit toolkit to convert SMILES strings into a 2D molecular graph. As shown in Figure 8, the text descriptions available to us contain detailed local descriptions of molecular structures. The corresponding parts of the text and molecular structures are highlighted with the same color in the table for clarity. Effectively utilizing these localized descriptions is crucial for enhancing the performance of text-based controlled molecule generation tasks. The result of our experiments offers substantial evidence supporting the significance of leveraging these fine-grained descriptions in the generation process.

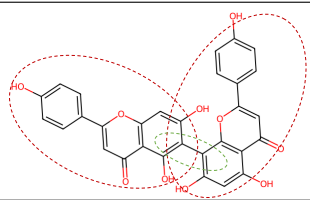
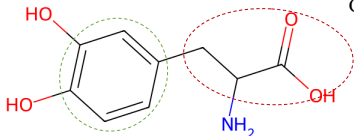
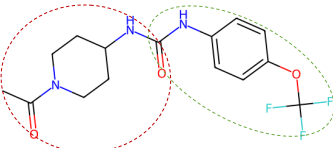
Molecule Graph	SMILES	Description
	<chem>C1=CC(=CC=C1C2=CC(=O)C3=C(O)C=C(C(=C3O)C4=C(C=C(C5=C4OC(=CC5=O)C6=CC=C(C(=C6O)O)O)O)O)O</chem>	The molecule is a biflavonoid that is obtained by oxidative coupling of two molecules of apigenin resulting in a bond between positions C-6 and C-8 of the two chromene rings. It has a role as an antineoplastic agent, an antiviral agent, a hepatoprotective agent and a metabolite. It is a biflavonoid, a hydroxyflavone and a biaryl.
	<chem>C1=CC(=C(C=C1CC(C(=O)O)N)O)O</chem>	The molecule is a hydroxyphenylalanine carrying hydroxy substituents at positions 3 and 4 of the benzene ring . It has a role as a human metabolite. It is a hydroxyphenylalanine, a tyrosine derivative and a non-proteinogenic alpha-amino acid.
	<chem>CC(=O)N1CCC(CC1)NC(=O)NC2=C(C=C(C=C2)OC(F)(F)F)F</chem>	The molecule is a phenylurea that is urea substituted by 1-acetyl piperidin-4-yl and 4-(trifluoromethoxy)phenyl groups at positions 1 and 3 respectively. It has a role as an EC 3.3.2.10 (soluble epoxide hydrolase) inhibitor.

Figure 8: Examples of dataset.

C Initial Training Details

C.1 Training Set Up

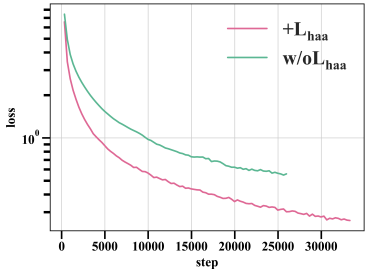
For the backbone models, we choose MolT5-base which is pre-trained in masked language modeling manner on two uni-modal datasets: natural language dataset and molecular dataset. For the model implementation, we use the PyTorch Lightning framework and employ distributed parallel training. We use the AdamW optimizer with no weight decay and the learning rate is set to $1e^{-4}$. The key hyperparameters used in Atomas are illustrated in the table Table 10.

Table 10: **Hyperparameter details for Atomas.**

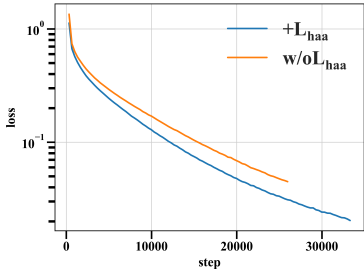
Hyperparameter	Value
batchsize	16
epoch	100
encoder learning rate	$1e^{-4}$
decoder learning rate	$1e^{-4}$
text projection learning rate	$1e^{-5}$
molecule projection learning rate	$1e^{-5}$
max padding length	512
queue size	13200
precision	BFloat16 Automatic Mixed Precision

C.2 Training Analysis

We visualized the loss curve for training 100 epochs during initial training. We scaled the loss value using a logarithmic scale. Figure 9a shows the loss curve of the global alignment \mathcal{L}_{ga} after the addition of hierarchical adaptive alignment loss \mathcal{L}_{haa} . Figure 9b shows the loss curve of language modeling \mathcal{L}_{lm} after the addition of the hierarchical adaptive alignment loss \mathcal{L}_{haa} . The observations suggest that the hierarchical adaptive alignment enhances global alignment and controllable generation.



(a) The convergence of \mathcal{L}_{ga} loss both in the absence and presence of \mathcal{L}_{haa} loss.



(b) The convergence of \mathcal{L}_{lm} loss both in the absence and presence of \mathcal{L}_{haa} loss

D Downstream Task Details

D.1 Metrics

Metrics of Zero-shot Molecule-Text Retrieval In retrieval task, we are consistent with the natural scene, using the most common search indicators in the natural scene (*i.e.*, text-image retrieval). Recall at 1/5/10 is a performance metric for information retrieval systems, such as search engines or recommendation systems, that measures the proportion of relevant results found within the top 1, 5, or 10 returned items, indicating the model’s effectiveness in retrieving pertinent information. MRR: mean reversed rank. MRR evaluates information retrieval model by averaging the inverse positions of the first relevant results across multiple queries, reflecting the model’s effectiveness in ranking relevant items.

Metrics of Molecule Captioning In molecule captioning task, we follow the MolT5 model and employ BLEU (Bilingual Evaluation Understudy) and ROUGE (Recall-Oriented Understudy for Gisting Evaluation) as evaluation metrics for captions. BLEU measures the overlap of n-grams between the generated text and the reference text. BLEU-n refers to the BLEU metric with n-grams, where n is an integer value (*e.g.*, 1 for unigrams, 2 for bigrams, 3 for trigrams). For example, BLEU-1 measures the accuracy of word level, and higher-order BLEU can measure the fluency of sentences. The BLEU score ranges between 0 and 1. A BLEU score of 0.6 or 0.7 is considered to be a good result. ROUGE-N measures the overlap of N-grams (*e.g.*, unigrams, bigrams, trigrams) between the generated and reference texts. It calculates precision, recall, and F-score for N-grams, providing a balanced assessment of the model’s performance. ROUGE-L is based on the longest common subsequence (LCS) between the generated and reference texts. It considers the longest continuous sequence of words that appear in both texts, capturing the overall coherence and flow of the generated text.

Metrics of Text-based de Novo Molecule Generation In molecule generation task we use BLEU, Exact, Levenshtein, MACCS FTS, RDK FTS, Morgan FTS, Validity 7 metric. Exact refers to the Exact Match metric measures the percentage of predictions that exactly match the true labels. The Levenshtein distance, also known as the edit distance, is a metric used to measure the similarity between two strings by calculating the minimum number of single-character edits (insertions, deletions, or substitutions) required to transform one string into the other. Validity refers to the percentage of molecules that can be processed by the RDKit and measures the grammatical normality of the generated molecules. MACCS FTS, RDK FTS and Morgan FTS are molecule fingerprint metrics.

D.2 Baselines

Baselines of Zero-shot Molecule-Text Retrieval MolFM jointly train three unimodal encoders, which separately encodes molecular structures, biomedical texts, and knowledge graphs to learn joint representations. MoMu [31] is a pre-trained model that utilizes contrastive learning to align molecular graphs with their corresponding text descriptions. KV-PLM [38] integrates molecular structure information with text-based knowledge, enabling the molecular structure to learn meta-knowledge from text through pre-training BERT’s Masked Language Model [12]. GraphMVP [19] fusion 2D topological structure and 3D geometric information through contrastive and generative pretext tasks.

Baselines of Molecule Captioning We compared 8 baselines including MoMu, MolXPT, GIT-Mol [18], MolFM, MolT5, MolReGPT, Text+Chem T5, InstructMol [2] and MolCA [22]. MolXPT is a GPT-like model that uses the GPT-2_{medium} configuration pre-trained on SMILES sequences wrapped by text. GIT-Mol maps molecular graphs, images, and text SMILES modalities into a unified latent space using a GIT-Former designed based on the Q-Former architecture in BLIP2 [15]. MolT5 is a T5-based text-to-text model, pre-trained on a large-scale single-modal corpus of natural language and molecules, thereby obtaining prior knowledge of the two domains. MolReGPT employs GPT-3.5-turbo and GPT-4-0314, and designs a retrieval-based prompt paradigm through in-context learning to improve molecule discovery without any additional training. Text+Chem T5 develops a multi-task, multi-domain model for natural and chemical language. InstructMol employs instruction-tuning manner through two-stage training to fine-tune LLMs (large language models). InstructMol+GS refers to the use of both molecular graph tokens and SMILES tokens as input. MolCA bridges molecular 2D graph and text by projecting the graph into a semantic space similar to text.

Baselines of Text-based de Novo Molecule Generation We compared the performance of six out of seven baselines used in molecule captioning task. We excluded the InstructMol method from the comparison, as it is not directly applicable to the molecule generation task.

E Ablation Study

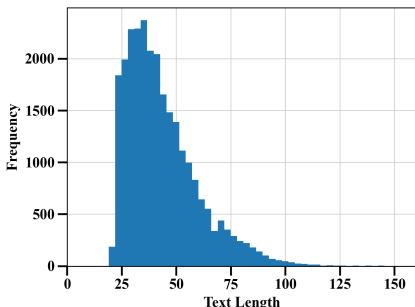
E.1 Ablation Study for Unified Encoder vs Separate Encoder

Table 11 presents the advantages of utilizing a unified encoder in the Atomas.

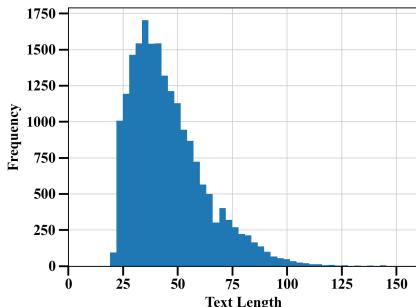
Figures 10a to 10d illustrates the distribution of the ChEBI-20 training data after weighted sampling. These data is utilized to verify that the unified encoder outperforms separate encoders in scenarios with limited data availability.

Table 11: **Ablation study for the use of the unified encoder and separate encoder.** Performance on the text-based de novo molecule generation task using the ChEBI-20 dataset. “↑” denotes that higher is better. “↓” denotes that lower is better.

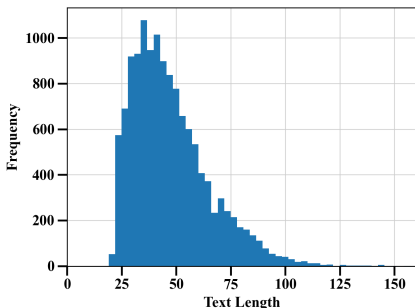
Method	BLEU↑	Exact↑	Levenshtein↓	MACCS FTS↑	RDKit FTS↑	Morgan FTS↑	Validity↑
Baseline	0.783	0.082	24.846	0.788	0.661	0.602	0.787
Sep-encoder	0.853	0.278	15.72	0.895	0.805	0.745	0.945
Uni-encoder	0.854	0.298	15.472	0.898	0.809	0.750	0.947



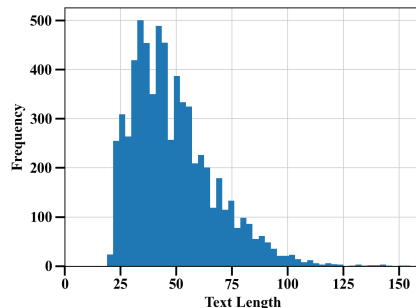
(a) The text length distribution of full ChEBI-20 training dataset.



(b) The distribution of text length in 75% of the ChEBI-20 training dataset after applying weighted sampling.



(c) The distribution of text length in 50% of the ChEBI-20 training dataset after applying weighted sampling.



(d) The distribution of text length in 25% of the ChEBI-20 training dataset after applying weighted sampling.

E.2 Ablation Study for the Effectiveness of Components.

Table 12 presents the complete results of the ablation study for the effectiveness of components.

Table 12: **Ablation study for the effectiveness of components.** Performance on the text-based de novo molecule generation task using the ChEBI-20 dataset. “ \uparrow ” denotes that higher is better. “ \downarrow ” denotes that lower is better.

\mathcal{L}_{ga}	\mathcal{L}_{haa}	\mathcal{L}_{lm}	BLEU \uparrow	Exact \uparrow	Levenshtein \downarrow	MACCS FTS \uparrow	RDKit FTS \uparrow	Morgan FTS \uparrow	Validity \uparrow
		\checkmark	0.783	0.082	24.846	0.788	0.661	0.602	0.787
\checkmark		\checkmark	0.841	0.223	16.946	0.886	0.784	0.716	0.954
	\checkmark	\checkmark	0.844	0.266	16.675	0.893	0.799	0.736	0.952
\checkmark	\checkmark	\checkmark	0.854	0.298	15.472	0.898	0.809	0.750	0.947

E.3 Ablation Study for the Effectiveness of Joint Optimization.

Table 13 presents the complete results of the ablation study for the effectiveness of joint optimization.

Table 13: **Ablation study for the effectiveness of joint optimization.** Performance on the text-based de novo molecule generation task using the ChEBI-20 dataset.

Method	BLEU \uparrow	Exact \uparrow	Levenshtein \downarrow	MACCS FTS \uparrow	RDKit FTS \uparrow	Morgan FTS \uparrow	Validity \uparrow
Baseline	0.783	0.082	24.846	0.788	0.661	0.602	0.787
2Stages	0.782	0.106	26.029	0.812	0.689	0.602	0.910
Jointly optimization	0.841	0.223	16.946	0.886	0.784	0.716	0.954

E.4 Ablation Study for the Effectiveness of Different Number of Hierarchical Alignment Levels.

Table 14 presents the complete results of the effect of different number of hierarchical alignment levels.

Table 14: **Ablation study for the effect of different number of hierarchical alignment levels.** Performance on the text-based de novo molecule generation task using the ChEBI-20 dataset.

Level Num	BLEU \uparrow	Exact \uparrow	Levenshtein \downarrow	MACCS FTS \uparrow	RDKit FTS \uparrow	Morgan FTS \uparrow	Validity \uparrow
0	0.841	0.223	16.946	0.886	0.784	0.716	0.954
2	0.854	0.289	15.506	0.896	0.805	0.746	0.950
3	0.854	0.298	15.472	0.898	0.809	0.750	0.947
4	0.852	0.287	15.580	0.897	0.808	0.746	0.952

F Case study

F.1 Molecule captioning

Figure 11 shows more molecule caption examples.

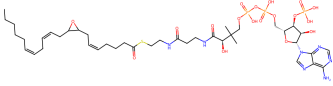
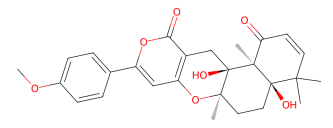
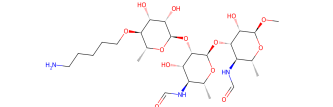
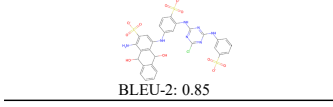
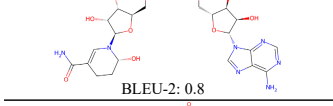

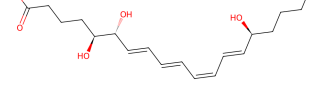
Molecule Input	Atomos Output	Ground Truth
 <p>BLEU-2: 1.0</p>	<p>The molecule is an unsaturated fatty acyl-CoA that results from the formal condensation of the thiol group of coenzyme A with the carboxy group of 8,9-epoxy-(5Z,11Z,14Z)-icosatrienoic acid. It is a long-chain fatty acyl-CoA and an unsaturated fatty acyl-CoA. It derives from an 8,9-EET. It is a conjugate acid of an 8,9-epoxy-(5Z,11Z,14Z)-icosatrienoyl-CoA(4-).</p>	<p>The molecule is an unsaturated fatty acyl-CoA that results from the formal condensation of the thiol group of coenzyme A with the carboxy group of 8,9-epoxy-(5Z,11Z,14Z)-icosatrienoic acid. It is a long-chain fatty acyl-CoA and an unsaturated fatty acyl-CoA. It derives from an 8,9-EET. It is a conjugate acid of an 8,9-epoxy-(5Z,11Z,14Z)-icosatrienoyl-CoA(4-).</p>
 <p>BLEU-2: 0.95</p>	<p>The molecule is an organophosphate oxoanion obtained by deprotonation of the carboxy and phosphate OH groups of (9S,10R)-10-hydroxy-9-(phosphonoxy)octadecanoic acid; major species at pH 7.3. It is an organophosphate oxoanion and a monocarboxylic acid anion. It is a conjugate base of a (9S,10R)-10-hydroxy-9-(phosphonoxy)octadecanoic acid.</p>	<p>The molecule is an organophosphate oxoanion obtained by deprotonation of the carboxy and phosphate OH groups of (9S,10R)-10-hydroxy-9-(phosphonoxy)octadecanoic acid; major species at pH 7.3. It is an organophosphate oxoanion and a hydroxy monocarboxylic acid anion. It is a conjugate base of a (9S,10R)-10-hydroxy-9-(phosphonoxy)octadecanoic acid.</p>
 <p>BLEU-2: 0.9</p>	<p>The molecule is a methyl glycoside that consists of a 4-O-(5-aminopentyl)-alpha-D-mannose residue and three N-formyl-alpha-D-perosamine residues linked sequentially (1->2), (1->3) and (1->2) and linked at the reducing end glycosidically to a methyl group. It is a methyl glycoside and a trisaccharide derivative.</p>	<p>The molecule is a methyl glycoside that consists of a 4-O-(5-aminopentyl)-alpha-D-mannose residue and two N-formyl-alpha-D-perosamine residues linked sequentially (1->2) and (1->3) and linked at the reducing end glycosidically to a methyl group. It is a methyl glycoside and a trisaccharide derivative.</p>
 <p>BLEU-2: 0.85</p>	<p>The molecule is the organosulfonate oxoanion that is the trianion of Reactive Blue 5, formed by loss of a proton from each of the sulfo groups; major species at pH 7.3. It is a conjugate base of a Reactive Blue 5.</p>	<p>The molecule is the organosulfonate oxoanion that is the trianion of Reactive Blue 5 quinol form, obtained by loss of a proton from each of the sulfo groups; major species at pH 7.3. It is a conjugate base of a Reactive Blue 5 quinol form.</p>
 <p>BLEU-2: 0.8</p>	<p>The molecule is a pyrrolizine alkaloid that is produced by a hybrid species of Jacobaea. It has a role as a Jacobaea metabolite. It is a pyrrolizine alkaloid, a tertiary amine oxide, a tertiary alcohol, a macrocyclic lactone, an organic heterotricyclic compound and a tertiary amine oxide. It derives from a Senecivermine.</p>	<p>The molecule is a pyrrolizine alkaloid that is jacoline in which the tertiary amino function has been oxidised to the corresponding N-oxide. It has a role as a Jacobaea metabolite. It is a macrocyclic lactone, an organic heterotricyclic compound, a pyrrolizine alkaloid, a triol and a tertiary amine oxide. It derives from a jacoline.</p>
 <p>BLEU-2: 0.7</p>	<p>The molecule is a pyrrolizine alkaloid that is produced by a hybrid species of Jacobaea. It has a role as a Jacobaea metabolite. It is a pyrrolizine alkaloid, a tertiary amine oxide, a tertiary alcohol, a macrocyclic lactone, an organic heterotricyclic compound and a tertiary amine oxide. It derives from a Senecivermine.</p>	<p>The molecule is a pyrrolizine alkaloid that is jacoline in which the tertiary amino function has been oxidised to the corresponding N-oxide. It has a role as a Jacobaea metabolite. It is a macrocyclic lactone, an organic heterotricyclic compound, a pyrrolizine alkaloid, a triol and a tertiary amine oxide. It derives from a jacoline.</p>
 <p>BLEU-2: 0.6</p>	<p>The molecule is a hydroxy fatty acid anion obtained by deprotonation of the carboxy function of lipoxin A4; major species at pH 7.3. It has a role as a human metabolite and a Saccharomyces cerevisiae metabolite. It is a hydroxy fatty acid anion, an icosanoid anion, a long-chain fatty acid anion and a polyunsaturated fatty acid anion. It is a conjugate base of a lipoxin A4.</p>	<p>The molecule is a hydroxy fatty acid anion obtained by deprotonation of the carboxy function of lipoxin A4; major species at pH 7.3. It is a hydroxy fatty acid anion and a lipoxin anion. It is a conjugate base of a lipoxin A4.</p>

Figure 11: Additional molecule captioning examples.

F.2 Text-based de Novo Molecule Generation

Figure 12 shows more text-based de novo molecule generation examples.

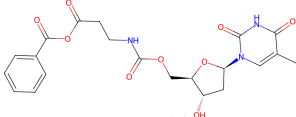
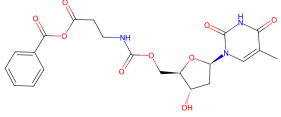
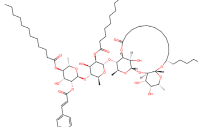
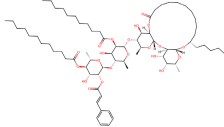
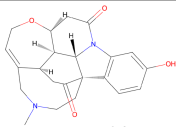
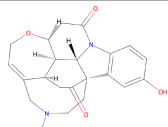
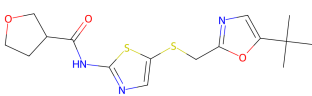
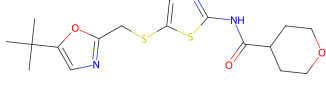
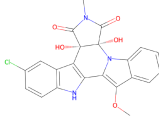
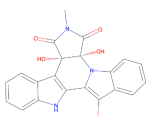
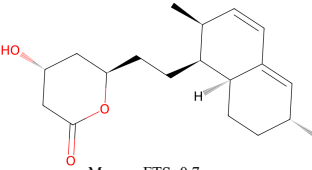
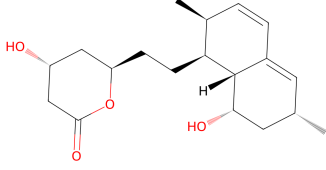
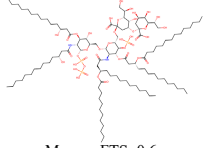
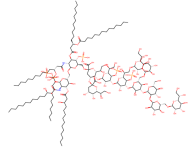
Text Input	Atomos Output	Ground Truth
The molecule is a carbamate ester of thymidine in which the 5'-hydroxy group has been esterified with [3-(benzoyloxy)-3-oxopropyl]carbamic acid. It derives from a thymidine.	 Morgan FTS: 1.0	
The molecule is a resin glycoside that is the tetrasaccharide derivative of jalapinolic acid. It has been isolated from Ipomoea batatas. It has a role as a metabolite. It is a cinnamate ester, a macrocyclic lactone, a resin glycoside, a tetrasaccharide derivative and a dodecanoate ester. It derives from a trans-cinnamic acid and a jalapinolic acid.	 Morgan FTS: 0.95	
The molecule is a monoterpenoid indole alkaloid with formula C ₂₂ H ₂₄ N ₂ O ₄ , originally isolated from the seeds of Strychnos nux-vomica. It has a role as a plant metabolite. It is a delta-lactam, a cyclic ketone, a monoterpenoid indole alkaloid, an organic heterohexacyclic compound, a tertiary amino compound and a member of phenols.	 Morgan FTS: 0.9	
The molecule is a secondary carboxamide resulting from the formal condensation of the carboxy group of tetrahydro-2H-pyran-4-carboxylic acid with the amino group of 5-[[[(5-tert-butyl-1,3-oxazol-2-yl)methyl]sulfanyl]-1,3-thiazol-2-amine. It is a CDK18 kinase inhibitor. It has a role as an EC 2.7.11.22 (cyclin-dependent kinase) inhibitor. It is a member of 1,3-oxazoles, a member of 1,3-thiazoles, an organic sulfide, a secondary carboxamide and a member of oxanes.	 Morgan FTS: 0.85	
The molecule is an organic heterohexacyclic compound that is cladoniamide B in which both of the chlorines are replaced by hydrogen. It has been isolated from the culture broth of Streptomyces uncialis. It is a cladoniamide, an organic heterohexacyclic compound, a dicarboximide, a tertiary alcohol and a diol.	 Morgan FTS: 0.8	
The molecule is a polyketide that is monacolin L bearing an additional hydroxy substituent at position 8. It has a role as an antimicrobial agent, a fungal metabolite and an EC 1.1.1.34/EC 1.1.1.88 (hydroxymethylglutaryl-CoA reductase) inhibitor. It is a secondary alcohol, a polyketide, a carbocyclic compound, a member of 2-pyranones and a member of hexahydronaphthalenes. It derives from a monacolin L.	 Morgan FTS: 0.7	
The molecule is a lipid A that is lipid A-core in which the anomeric phosphate is replaced by a diphosphate. It is a member of lipid As, a dodecanoate ester and a tetradecanoate ester. It is a conjugate acid of a lipid A-core 1-diphosphate(11-).	 Morgan FTS: 0.6	

Figure 12: Additional text-based de novo molecule generation examples.